

METAMORPHISM OF THE ULTRAMAFIC ROCKS OF THE THOMPSON MINE, THOMPSON NICKEL BELT, NORTHERN MANITOBA*

A. DOĞAN PAKTUŇ

Department of Geology, University of Ottawa, Ottawa, Ontario K1N 6N5

ABSTRACT

Abundant sill-like bodies of serpentized ultramafic rocks, associated with nickel sulfide deposits, are found on the western side of the Thompson Nickel Belt (Manitoba), near the Moak-Setting Lakes cataclastic fault-zone. An unusually fresh ultramafic body, found on the 4000 level of the Thompson mine, is composed of dunitic, peridotitic, orthopyroxenitic and amphibolitic units. Tremolite is present as a Ca-bearing silicate in most of these rocks. The Mg/(Mg + Fe) ratio of olivine ranges from 0.83 to 0.90, whereas that of orthopyroxene ranges from 0.85 to 0.91 as a function of the bulk-rock chemistry. Spinel ranges in composition from Al-chromite to Mg-Al-spinel as the grade of metamorphism increases. The ultramafic body was partly altered before being progressively metamorphosed under upper-amphibolite-facies conditions. The approximate maximum temperature attained during metamorphism is estimated to be 700°C. The body was subsequently deformed. Recrystallization processes, which resulted in the formation of equigranular mosaics of olivine neoblasts, followed the deformational episode. Late-stage shearing and retrograde metamorphism led to secondary chlorite and thin veins of serpentine developed locally parallel to the fabric, along the margins of the ultramafic body.

Keywords: metamorphism, ultramafic rocks, nickel sulfide deposit, Thompson, Manitoba.

SOMMAIRE

On trouve d'abondants massifs du type filon-couche de roches ultramafiques serpentinisées, associés à des dépôts de nickel sur le côté Ouest de la ceinture nickélicifère de Thompson (Manitoba), près de la zone de faille cataclastique des lacs Moak-Setting. Un massif ultramafique très peu altéré, observé au niveau 4000 de la mine Thompson, se compose d'unités dunitiques, péridotitiques, orthopyroxénitiques et amphibolitiques. La trémolite est présente comme minéral calcifère dans la plupart de ces roches. Le rapport Mg/(Mg + Fe) de l'olivine varie de 0.83 à 0.90, alors que celui de l'orthopyroxène varie de 0.85 à 0.91 en fonction du chimisme global de la roche. En composition, le spinelle passe de la chromite alumineuse au spinelle-Mg-Al quand augmente l'intensité du métamorphisme. Le massif ultramafique fut partiellement altéré avant d'être graduellement métamorphosé au faciès amphibolite supérieur. Les roches ont atteint une température maximum d'environ 700°C au cours du métamorphisme. Le massif se

déforma par la suite. Les processus de recristallisation responsables de la formation de mosaïques équi-granulaires de néoblastes d'olivine suivirent l'épisode de déformation. Le cisaillement tardif et le métamorphisme rétrograde sont marqués par la chlorite secondaire et les filonnets de serpentine que l'on trouve développés localement parallèlement à la fabrique, en bordure du massif ultramafique. (Traduit par la Rédaction)

Mots-clés: métamorphisme, roches ultramafiques, gisements de sulfures de nickel, Thompson, Manitoba.

INTRODUCTION

The Thompson Nickel Belt lies on the boundary between the Churchill and the Superior provinces in north-central Manitoba (Fig. 1). The Moak - Setting Lakes cataclastic fault-zone defines the northwestern boundary with the Churchill Province. The southeastern boundary, on the other hand, is partly a cataclastic fault-zone and partly a zone of metamorphic transition (Cranstone & Turek 1976) that defines the border with the Pikwitonei Province. In addition to the structural importance of this belt, it contains important deposits of nickel sulfide; therefore, the belt has been mapped in detail, and various aspects have been studied. A comprehensive geological outline of the belt is given by Peredery (1982).

Ultramafic rocks occur close to the northwestern side of the belt. Individual bodies have been studied by various workers: the bodies of the Manibridge mine by Coats (1966), those located on the southwestern edge of the belt, under the Paleozoic cover by Bliss (1973), and the Pipe II and West Manasan ultramafic bodies by Saboia (1978). Generally they are extensively serpentized and sheared, retaining very little relict texture.

In this study, ultramafic rocks from the different levels of the Thompson mine have been investigated. However, special attention is given to a large ultramafic body found at the 4000 level since it is remarkably fresh compared to the other ultramafic bodies found in the belt.

GENERAL GEOLOGY

The belt is underlain predominantly by migmatitic

*Publication 25-83, Ottawa-Carleton Centre for Geoscience Studies.

gneisses that mainly contain amphibolite-facies mineral assemblages. However, granulite-facies assemblages are also common in the belt and are interpreted by Weber & Scoates (1978), Peredery (1979) and Russell (1981) as relict Archean granulites that survived the Hudsonian Orogeny.

Near the western margin of the belt, the basement gneisses are overlain by thin (150–1500 m) Aphebian supracrustal rocks (Peredery 1982) that include metasedimentary and metavolcanic assemblages. These exhibit a range of metamorphic grades from middle amphibolite to granulite. Two metasedimentary assemblages, the Pipe and Thompson groups, have been distinguished on the basis of lithology and metamorphic grade (Peredery 1982). The Thompson metasediments show a higher metamorphic grade and include quartzite, skarn, iron formation and schist.

These supracrustal rocks and the basement gneisses were intruded by abundant ultramafic and mafic sills and dykes. Ultramafic bodies are generally lenseoid or tabular in shape and vary in width from several metres to several hundreds of metres. The contact between the ultramafic bodies and the enclosing rocks is usually conformable, but the contact rocks are so deformed and altered that their true character is uncertain (Peredery 1982). Ultramafic rocks range in composition from peridotite to pyroxenite and are extensively altered. Peredery (1979) also used a field term, 'ultramafic amphibolite', to describe a variety of ultramafic rocks that ranges in composition from picrite to pyroxenite.

In the Thompson mine, nickel sulfides are found mainly as massive sulfide bodies together with ultramafic rocks in the metasedimentary rocks. Ultramafic rocks are mainly in the form of inclu-

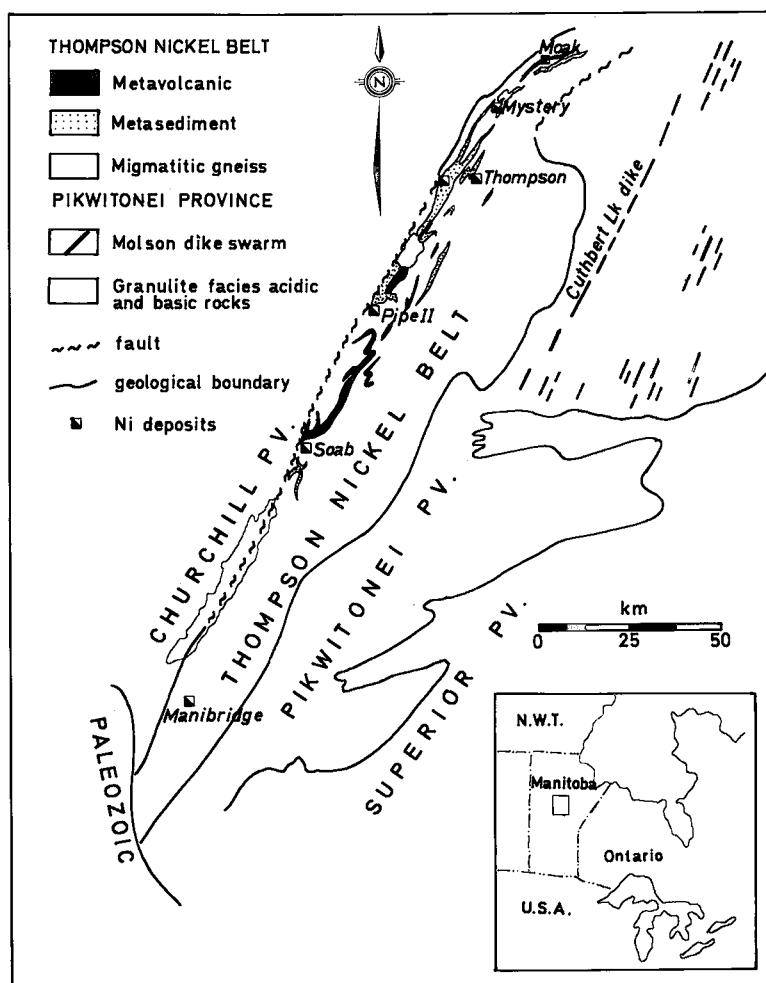


FIG. 1. Regional setting of the Thompson Nickel Belt.

sions, which range in size up to several metres across, in massive sulfides. Although larger ultramafic bodies are not uncommon in the Thompson mine, their volume is small relative to the amount of sulfides.

Nickel sulfide deposits of the Pipe II mine, Mystery and Moak localities mainly occur in the form of disseminated sulfides in the ultramafic rocks. According to Peredery (1982), the distribution of sulfides is largely the result of remobilization during the complex tectonic and metamorphic history of the belt.

The major structure of the Thompson mine is an anticlinal fold striking northeast and plunging steeply to the south, according to Zurbrigg (1963). However, the fold could be synclinal, judging from similarities in stratigraphic succession between the

Thompson and Pipe sedimentary sequences, according to Peredery (1982). Cross folding, with an axial trend close to north-south, accounts for the configuration of the Thompson Group of metasedimentary rocks (Peredery 1982). The earlier folds are subhorizontal, and their axial plane strikes north-northeast.

MINERALOGY AND PETROGRAPHY

The ultramafic body at the 4000 level of the Thompson mine, as seen along two drill holes (Fig. 2), is 130 metres thick, probably lensoid in shape and enclosed in a garnet-sillimanite-biotite schist. The body is composed of peridotitic, orthopyroxenitic and amphibolitic rocks. Using the scheme of Evans (1977), the mineral assemblages correspond to

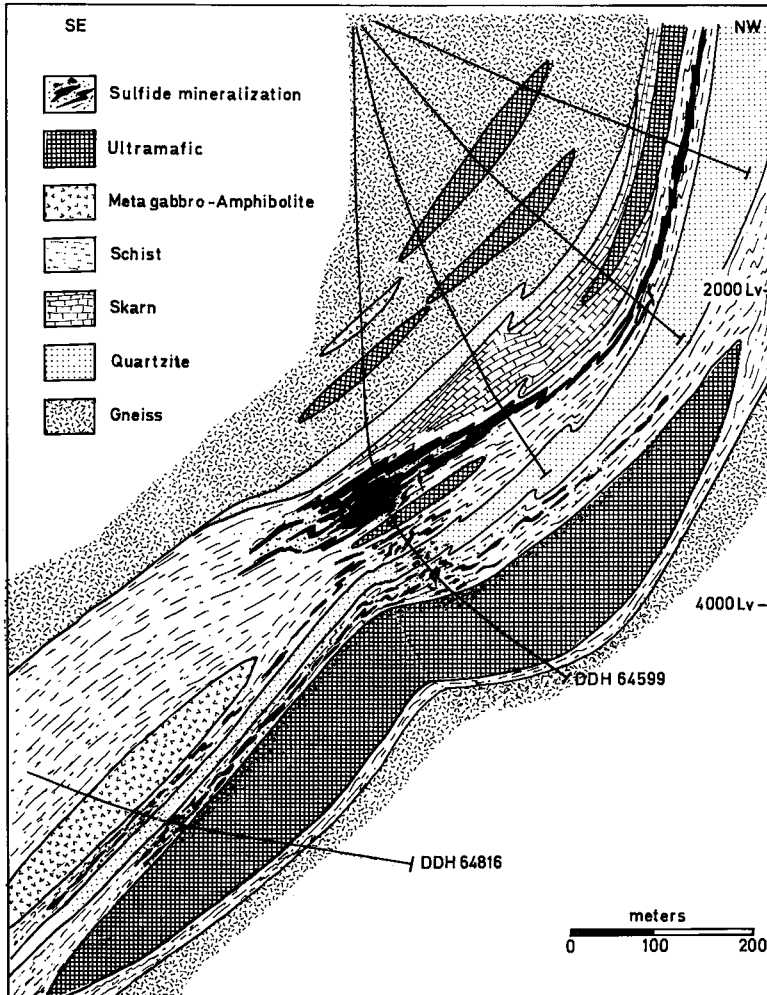


FIG. 2. 3600 N vertical section of the Thompson mine (T-3).

tremolite peridotite and tremolite pyroxenite (Fig. 3), which are indicative of the amphibolite facies. The unit named 'amphibole-rich pyroxenite' in Figure 3 is mineralogically similar to the ultramafic amphibolite of Peredery (1979). The main sulfide mineralization is found in the enclosing schist in the form of massive and stringer ore. Minor disseminations of sulfides are present in the ultramafic body, close to its contact with mineralized schist. As observed in core from drill hole 64599, tremolite peridotite and its serpentinized equivalents amount to one half of the body, whereas the tremolite pyroxenite makes up more than one third (Fig. 3). Tremolite-olivine pyroxenite is the main rock type seen along drill hole 64816.

Tremolite peridotite

Olivine in the peridotitic zones is of two types: megacrystic (2–4 mm) and fine grained (less than 1 mm). Megacrystic olivine usually is black owing to fine opaque dusty material disseminated or concentrated along irregular fractures in olivine (Fig. 4). This material, possibly magnetite, may be the product of high-temperature oxidation of olivine (Haggerty & Baker 1967, Champness 1970, Putnis 1979).

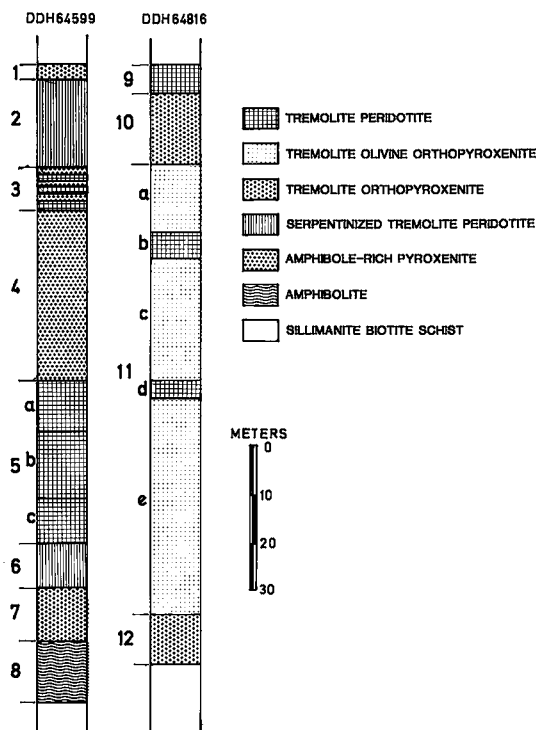


FIG. 3. Nature of the ultramafic body, as observed in two diamond-drill holes.

Alternately, it may be magnetite formed during a previous episode of serpentinization and included in metamorphic olivine during progressive metamorphism (Arai 1975, Vance & Dungan 1977). A similar texture, consisting of black olivine megacrysts with dense tiny ilmenite granules, occurring in the outermost zone of the Bergell aureole in the Malenco serpentinite, is described by Trommsdorff & Evans (1980). Fluid and fine solid inclusions are commonly associated with the dusty material (Fig. 4). Pale brown to brownish yellow, euhedral to subhedral solid inclusions are probably spinel. Some of the olivine megacrysts display undulatory extinction and kink banding (Fig. 5).

Small light green grains of olivine, on the other hand, do not contain opaque dusty material and are strain-free. This variety forms an equigranular sugary mosaic texture that is well developed in zone 5b (Fig. 6). Among these grains, 120° interfacial angles are commonly seen (Fig. 7). Textural relations indicate that these fine grains of olivine are formed from megacrystic olivine by recrystallization processes. Recrystallization starts along grain boundaries and dislocations (Figs. 5, 8). This new generation of olivine is called *neoblast*, following the terminology advocated by Mercier & Nicolas (1975) for deformed upper-mantle peridotites.

Peridotite in zone 5a consists of loosely packed olivine megacrysts, neoblastic olivine mosaic and a light green-grey orthopyroxene-amphibole matrix, giving the rock a 'spotted' appearance. Dunite in zone 5c, on the other hand, is composed of closely packed megacrysts of olivine with a minimum of interstitial area (occupied by orthopyroxene, amphibole and aluminian chromite), with a texture very similar to the cumulus texture (Fig. 9). These equigranular olivine megacrysts very commonly enclose tiny subhedral inclusions of amphibole and chlorite, forming parallel oriented flakes or bunches

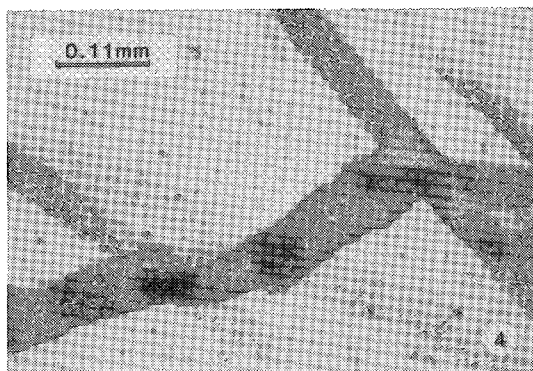


FIG. 4. Fine opaque dusty material concentrated along irregular fractures in olivine. Also shown are fluid and fine solid inclusions disseminated and concentrated along microfractures in olivine. Plane-polarized light.

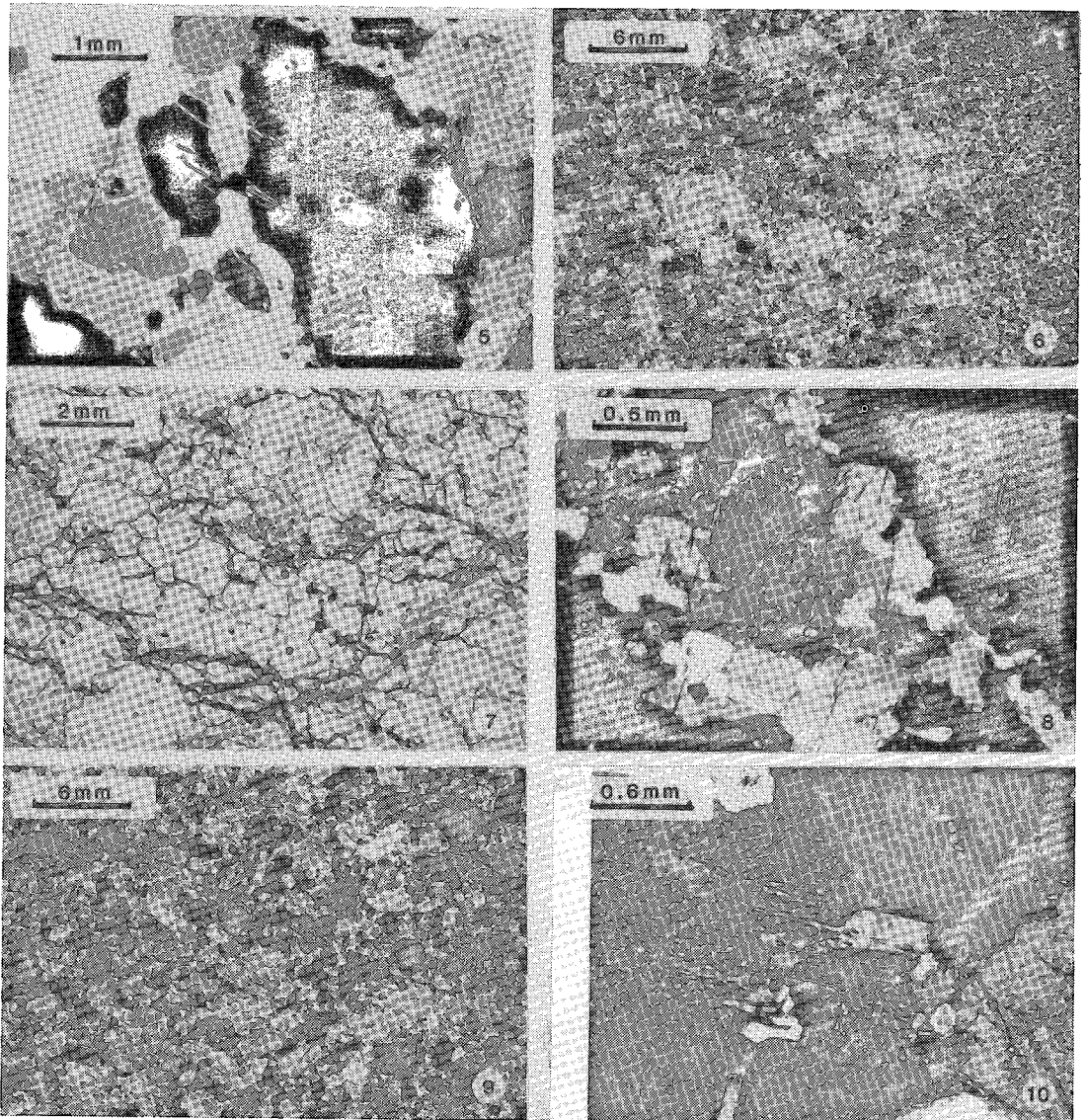


FIG. 5. Kink-banding (black and dark grey horizontal bands) in olivine megacryst. Parallel oriented flakes are amphibole and chlorite. Crossed polarizers.

FIG. 6. Neoblastic olivine occurring with megacrystic olivine from which it was derived. The megacrystic olivine completely recrystallized into neoblasts, forming a fine-grained mosaic texture on the right-hand side of the photomicrograph. Crossed polarizers.

FIG. 7. Fine-grained neoblastic olivine occurring together with orthopyroxene megacrysts. Idioblastic flakes are chlorite. Plane-polarized light.

FIG. 8. Large olivine megacryst containing olivine neoblasts, presumably developed along dislocation planes. Crossed polarizers.

FIG. 9. Closely packed olivine megacrysts forming cumulus texture. Crossed polarizers.

FIG. 10. Secondary chlorite developing along a preferred crystallographic direction of olivine megacryst, probably as a result of olivine and spinel reaction. Small relics of spinel are enclosed in chlorite. Crossed polarizers.

(Fig. 5) that are similar to those constituting the matrix. Close to the serpentinized tremolite peridotite (zone 6), there are anhedral chlorite inclusions in megacrystic olivine. It seems that they develop along certain crystallographic directions of the host olivine and usually enclose greenish yellow spinel (Fig. 10).

Tremolite peridotite in zones 2 and 6 is serpentinized, the degree of serpentinization varying throughout the zones. Thin serpentine veins form planar systems of veinlets probably parallel to the fabric of the body and the foliation of the enclosing schist. They cut megacrystic and neoblastic olivine and tremolite. Magnetite occurs in stringers following serpentine veins and along the cleavages of chlorite. Minor carbonate is also present in thin veins of serpentine.

Medium-grained orthopyroxene is found interstitially to olivine megacrysts, enclosing xenomorphic islands of olivine showing communal extinction (Fig.

11), and enclosing medium-grained amphibole and chlorite. Amphiboles are mainly colorless tremolite and cummingtonite. They generally form small fibrous and prismatic crystals, coexisting with olivine neoblasts.

Two types of spinel are present. One is pale brownish yellow chromian spinel, which is commonly seen as fine disseminated grains in the olivine orthopyroxenite and orthopyroxenite units. It is randomly disseminated throughout the peridotitic zones. In some places, however, it is preferentially concentrated along the grain boundaries of olivine megacrysts. The spinel usually forms fine anhedral zoned grains, the core of which is darker than the rim. The other type of spinel is opaque aluminian chromite, which is coarser than the first type. It occurs interstitially to the olivine megacrysts in zone 5b, in which the olivine grains are closely packed, forming a cumulus texture (Fig. 12).

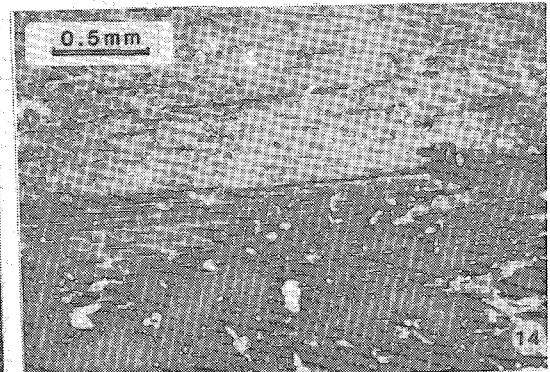
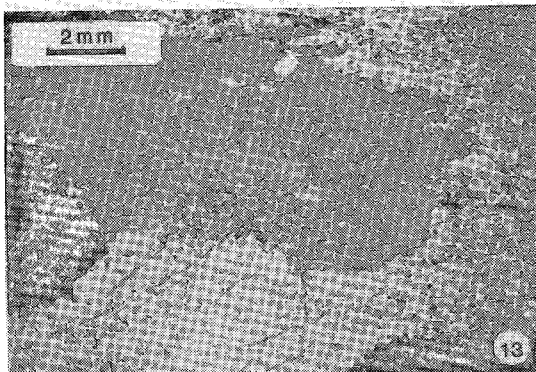
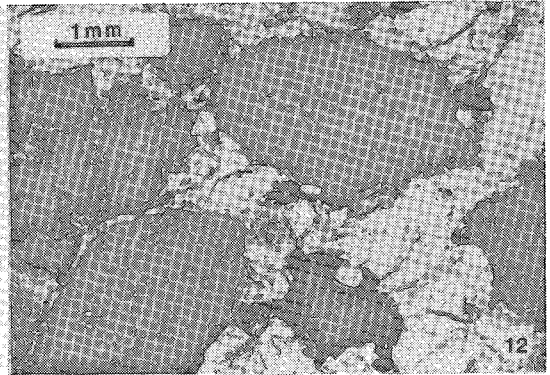
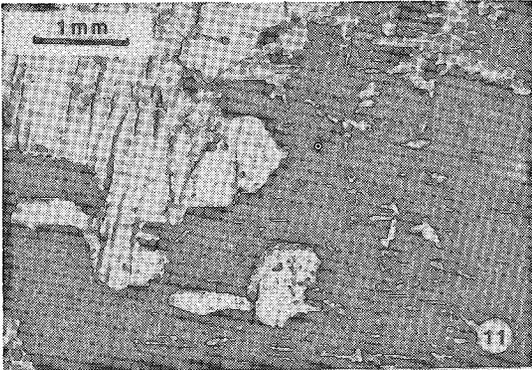


FIG. 11. Orthopyroxene (at extinction) replacing olivine megacryst. Crossed polarizers.

FIG. 12. Euhedral and subhedral olivine megacrysts. Al-chromite and minor orthopyroxene are interstitial to olivine. Crossed polarizers.

FIG. 13. Elongate orthopyroxene megacrysts enclosing fine inclusions similar to those constituting matrix. Crossed polarizers.

FIG. 14. Deformation lamellae in orthopyroxene. Crossed polarizers.

Tremolite orthopyroxenite

Orthopyroxene forms coarse, slightly elongate equigranular grains. Its grain size ranges from 0.3 to 1 cm, and it is pale brown. Abundant fine-grained amphibole, phlogopite and brown spinel are disseminated in some of the orthopyroxene megacrysts. The interstices of the orthopyroxene megacrysts are occupied by fine-grained light green amphibole and phlogopite, which are similar to those enclosed in the orthopyroxene but coarser in grain size (Fig. 13). Thin lamellae parallel to (100) of orthopyroxene are observed in some grains and characterized by a very low Ca content (Fig. 11, 14). Strained crystals of orthopyroxene are common. The orthopyroxene megacrysts in zone 1 are elongate, probably along the foliation plane of the enclosing schist. Tremolite is common as medium- to coarse-grained xenoblasts, whereas anthophyllite forms randomly oriented, radiating prismatic blade-like crystals in a finer-grained matrix. Phlogopite occurs as strained platy and fine grains. It is partly replaced by orthopyroxene in zone 1. In zone 12, on the margin of the body, phlogopite is recrystallized and replaced by a pseudomorph of green chlorite. Close to zone 3, minor olivine is present as small inclusions in orthopyroxene. Brown to greenish yellow spinel is very

common as small subhedral to anhedral crystals; these commonly are zoned (brownish core, yellow rim) disseminated grains, preferentially concentrated in the interstices of orthopyroxene megacrysts or in orthopyroxene close to its margins. Sulfides are present as disseminated anhedral grains.

Tremolite olivine orthopyroxenite

Texture is quite uniform in this unit. The grain size of olivine is 4 mm and less, and it forms xenomorphic grains that are usually enclosed in coarser (1-1.5 cm) orthopyroxene. Some of these orthopyroxene grains have triple junctions showing 120° interfacial angles.

Amphibolite

The unit in zone 8 is composed of amphibole, phlogopite and minor plagioclase. Amphibole forms a medium-grained (1 mm) granular texture with a weak fabric. Two amphiboles are present: magnesian cummingtonite and anthophyllite. Medium-grained phlogopite forms the groundmass for equigranular amphibole, and shows a foliation parallel to the margin of the body. Plagioclase, on the other hand, is fine- to medium-grained, occur-

TABLE 1. REPRESENTATIVE COMPOSITIONS OF OLIVINE, ORTHOPYROXENE AND SPINEL

	Olivine				Orthopyroxene				Spinel				
	1	2	3	4	1	2	3	4	1	2	3	4	5
SiO ₂	39.19	39.64	40.48	39.68	57.59	56.75	58.05	56.30	0.0	0.0	0.0	0.0	0.0
TiO ₂	0.0	0.0	0.0	0.0	0.0	0.0	0.06	0.09	0.0	0.0	0.0	0.05	0.27
Al ₂ O ₃	0.0	0.0	0.0	0.0	0.57	1.36	0.68	1.06	58.78	51.22	49.30	37.84	14.58
Cr ₂ O ₃	0.0	0.0	0.0	0.0	0.0	0.10	0.11	0.18	9.12	15.36	19.54	30.75	53.28
V ₂ O ₃									0.20	0.57	0.0	0.98	1.18
Fe ₂ O ₃									0.35	0.11	0.20	0.39	0.15
FeO	14.23	12.89	10.85	10.19	6.59	9.48	7.11	8.65	10.76	20.30	14.20	17.77	23.37
MgO	45.70	47.20	47.86	48.64	34.88	32.78	34.17	33.09	19.72	12.80	16.46	12.65	6.82
CaO	0.0	0.0	0.0	0.0	0.13	0.15	0.13	0.19	0.71	0.0	0.0	0.0	0.0
MnO	0.28	0.18	0.21	0.24	0.20	0.30	0.30	0.35	0.14	0.23	0.07	0.23	0.54
NiO	0.08	0.12	0.27	0.27	0.07	0.0	0.0	0.0	0.30	0.0	0.0	0.09	0.0
K ₂ O					0.0	0.0	0.0	0.0					
Na ₂ O					0.0	0.0	0.11	0.05					
TOTAL	99.48	100.03	99.67	99.20	100.03	100.92	100.72	99.96	100.08	100.59	99.97	100.76	100.19
X _{Mg}	0.851	0.867	0.887	0.895	0.904	0.860	0.895	0.872	0.766	0.529	0.674	0.559	0.342
Y _{Cr}									0.094	0.167	0.210	0.351	0.709

FeO represents total iron for olivine and orthopyroxene. Ferric iron is calculated assuming perfect stoichiometry for spinel. Olivine 1, 2: neoblasts; 3, 4: megacrysts. Spinel 1: brown, 2: yellowish brown, 3: red, 4: semiopaque, 5: opaque.

ring in the interstices between phlogopite and amphibole. This unit is cut by several thin (up to 1 cm) pegmatite veins.

MINERAL CHEMISTRY

Mineral analysis was performed with a Cambridge Mark V electron microprobe at the Department of

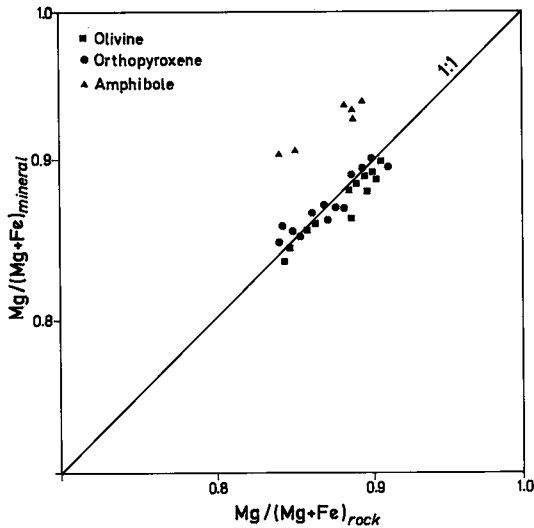


FIG. 15. Relationship of bulk-rock chemistry to the constituting minerals.

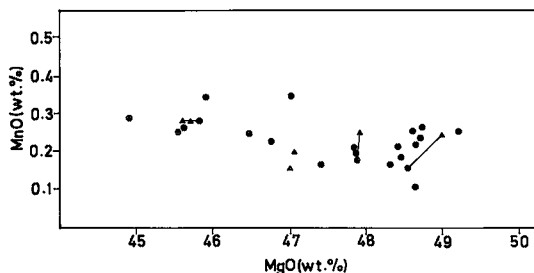
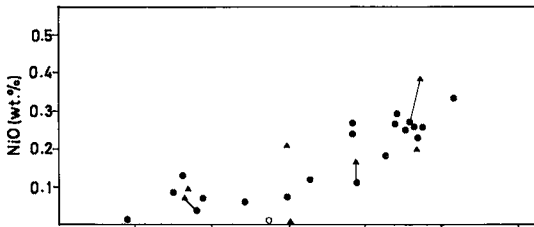


FIG. 16. Plots of MgO versus NiO and MnO (wt. %) in olivine. Tie-lines connect neoblastic olivine (triangles) to megacrystic olivine (solid circles) from which it was derived.

Geology, Dalhousie University. The instrument is equipped with an Ortec energy-dispersion spectrometer automated to produce simultaneous multielement analyses and reduce data using the program 'EDATA 2' of Smith & Gold (1979). Natural and synthetic minerals were used as standards. Several representative compositions of olivine, pyroxene and spinel from the ultramafic rocks described above are listed in Table 1. The complete set of analytical results, together with the precision of the analyses obtained from replicate determinations, are available on request from the Depository of Unpublished Data, CISTI, National Research Council of Canada, Ottawa, Ontario K1A 0S2.

Olivine

The composition of olivine in the dunitic zone 5b is uniform, ranging from Fo₈₈ to Fo₈₉. However, it is not uniform in zone 5a, and exhibits a rapid change from Fo₈₉ to Fo₈₅ toward zone 4. In zone 3, it is slightly more magnesian, Fo_{89.5}. The olivine from drill hole 64816 is more iron-rich, showing a compositional range from Fo₈₃ to Fo₈₇. This compositional variation is controlled mainly by the bulk-rock composition (Fig. 15). The NiO content of olivine ranges from the limit of detection to 0.40 wt. %, increasing with the magnesium content (Fig. 16). However, this relationship is not the same as shown by magmatic olivine. The olivine compositions with low nickel content fall outside the range defined by olivine in cumulates and mantle peridotites. The MnO content ranges from 0.1 to 0.35 wt. % and shows weak negative correlation with forsterite content.

The compositional difference between megacrystic and neoblastic varieties is small, although neoblastic olivine seems to be enriched in Ni and Mn compared to the megacrystic olivine from which it formed (Fig. 16). The individual grains of olivine megacrysts seem to be compositionally homogeneous.

Orthopyroxene

The Mg/(Mg + Fe) ratio (X_{Mg}) of orthopyroxene ranges from 0.84 to 0.91. It is 0.89 in zone 5b and decreases to 0.865 in zone 5a, showing a similar pattern to the X_{Mg} value of olivine. In zone 4, this ratio is about 0.85 and shows an increase toward zone 3. It reaches a maximum value of 0.905 in zone 3 (close to zone 4) and decreases toward zone 2. The orthopyroxene from zones 11 and 12 is more iron-rich, ranging from En₈₅ to En₈₇, similar to the coexisting olivine (Fo₈₃-Fo₈₇). The X_{Mg} of both olivine and orthopyroxene is probably controlled by the bulk-rock chemistry (Fig. 15).

The distribution coefficient for Mg and Fe between coexisting olivine and orthopyroxene [$K_D =$

$(X_{Mg}/X_{Fe})_{ol} \times (X_{Fe}/X_{Mg})_{opx}$] is 0.985 (Fig. 17). This is similar to the value for regionally metamorphosed peridotites from the Alps (0.96: Trommsdorff & Evans 1974) and smaller than those of zone IV of the Tari-Misaka contact-metamorphosed ultramafic complex (1.03: Arai 1975), Totalp serpentinites (1.05: Peters 1968) and metaperidotites of Paddy-Go-Easy Pass (1.10: Frost 1975). According to Medaris (1969), Mg and Fe partitioning between olivine and orthopyroxene is not sensitive to temperature over the range 700°C to 1300°C. However, recent thermodynamic formulations (Sack 1980) show that it is potentially a useful geothermometer.

Ca concentrations in orthopyroxene are very low (less than 0.21 wt.% CaO), similar to orthopyroxene from contact metamorphosed (Arai 1975) and regionally metamorphosed peridotites (Evans & Trommsdorff 1974). The Al content of orthopyroxene, here less than 1.75 wt.% Al_2O_3 , has been shown to be essentially a function of temperature (Dobretsov 1968, Fujii 1976, Mercier 1976) and of coexisting minerals. Its pressure dependence is restricted to temperatures above 900°C according to the T-P phase diagram of Gasparik & Lindsley (1980). Low contents of aluminum and calcium are characteristics of orthopyroxene in the amphibolite facies, though there is a gradual increase in these components as the higher-temperature parts of the facies are reached (Evans 1977). Highly aluminous orthopyroxene, on the other hand, is well known in alpine spinel peridotites equilibrated in the granulite facies (Evans 1977).

Amphibole

Calcic amphibole compositions plot between tremolite and pargasite end-members, forming a linear trend on the $^{iv}Al-(Na+K)$ diagram (Fig. 18) in the field of metamorphic amphiboles defined by Jamieson (1981). Al_2O_3 content ranges from 3.3 to 8.4% (wt.), increasing with an increase in alkali content. The CaO content is relatively constant at about 12.5 (wt.%)%. The Mg/(Mg+Fe) ratio of calcic amphibole ranges from 0.90 to 0.94 and is higher than that of the coexisting olivine and orthopyroxene (Fig. 17) and of the bulk rock (Fig. 15).

Spinel

In the peridotitic parts of the body, spinel ranges in composition from aluminian chromite to chromian spinel, whereas in the pyroxenitic parts it ranges from chromian spinel to Mg-Al-spinel. According to Evans (1977), these compositional ranges are confined close to the transition between the granulite and pyroxene-hornfels facies. Evans also indicated that the spinel is chromian magnetite in low-grade serpen-

tinities, ferritchromite in antigorite serpentinites and chromite in talc-olivine rocks.

The ratio $Cr/(Cr+Al+Fe^{3+})$, labeled Y_{Cr} , falls between 0.60 to 0.75 in the dunitic part of zone 5b and ranges from 0.10 to 0.75 in the rest of zone 5. Some of this wide range is defined by zoned grains and by grains in the same section. The rim of zoned grains is enriched in Al and Mg relative to Cr and Fe^{2+} (Fig. 19). Similar paths from core to rim are

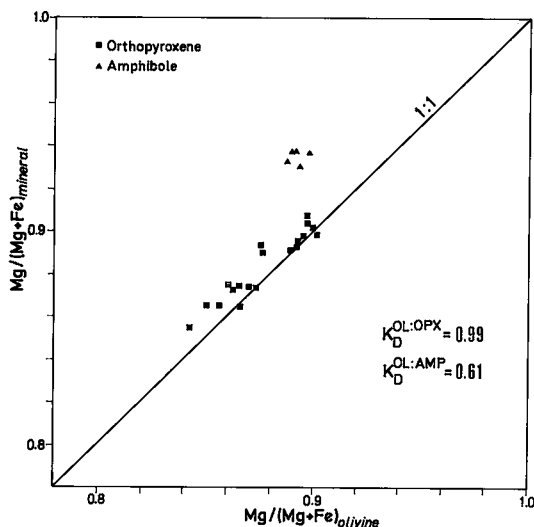


FIG. 17. Distribution of Mg and Fe between olivine and coexisting silicates.

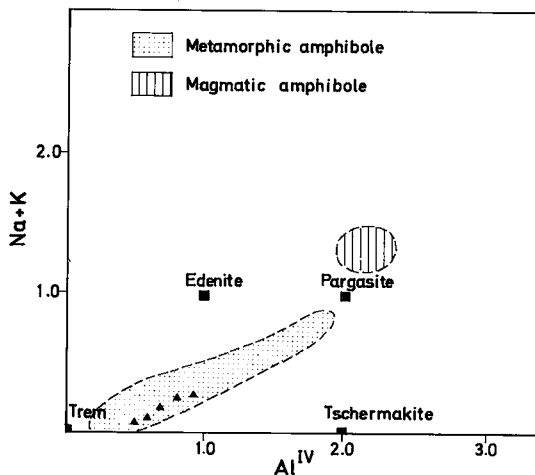


FIG. 18. Plot of ^{iv}Al versus $Na+K$ (number of atoms per 23 oxygen atoms) in calcic amphibole. Location of end-member compositions are after Deer *et al.* (1966). Fields of metamorphic and magmatic amphibole are those of Jamieson (1981).

reported by Evans & Frost (1975). This ratio is rather uniform in zone 4, ranging from 0.10 to 0.20.

The effect of temperature on Y_{Cr} of spinel and the Mg-Fe²⁺ partition between spinel and coexisting silicates was first studied by Irvine (1965), then by Evans & Frost (1975) and Frost (1975). In general, spinel becomes more Al- and Mg-rich relative to Cr and Fe²⁺, similar to the path seen in Figure 19, as the grade of metamorphism increases.

Minor elements such as Ti, V and Mn are enriched in Cr-rich varieties (Fig. 20). No such correlation exists for Ni. TiO₂ goes up to 0.30 wt.%, whereas V₂O₃ is less than 1.90 wt. %.

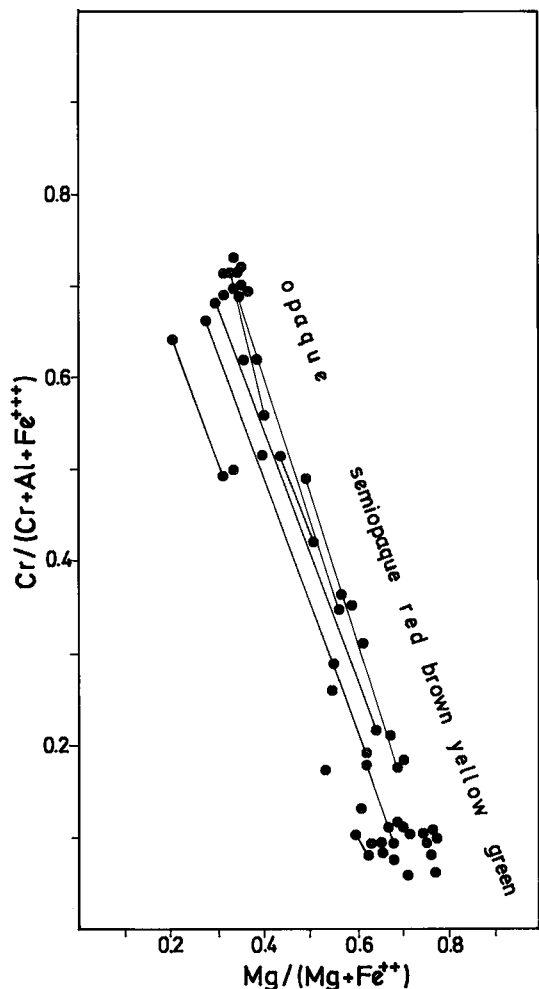


FIG. 19. Plot of X_{Mg} versus Y_{Cr} in spinel. $X_{Mg} = Mg/(Mg + Fe^{2+})$, $Y_{Cr} = Cr/(Cr + Al + Fe^{3+})$. Core and rim compositions of zoned spinel grains are connected. Spinel changes from opaque to green as the temperature increases.

GEOTEMPERATURE ESTIMATES

Olivine-spinel geothermometry based on the partition of Mg and Fe²⁺ between coexisting spinel and olivine has been applied to pairs from Thompson. Two different calibrations of this geothermometer have been used. One of them, that of Roeder *et al.* (1979), is basically the geothermometer of Jackson (1969) except that a different value for the free energy of FeCr₂O₄ has been used. The other is that of Fabriès (1979), which is based on the tentative graphical calibration of Evans & Frost (1975).

Temperatures obtained from these two calibrations are different. Those obtained from the equation of Roeder *et al.* (1979) vary from 400°C for Cr-rich spinel to 1100°C for Al-rich spinel. These temperatures are unreasonable for the mineral assemblages. The applicability of the Roeder *et al.* (1979) geothermometer has been challenged, since their isotherms are inconsistent with recently determined reversed experimental data at low

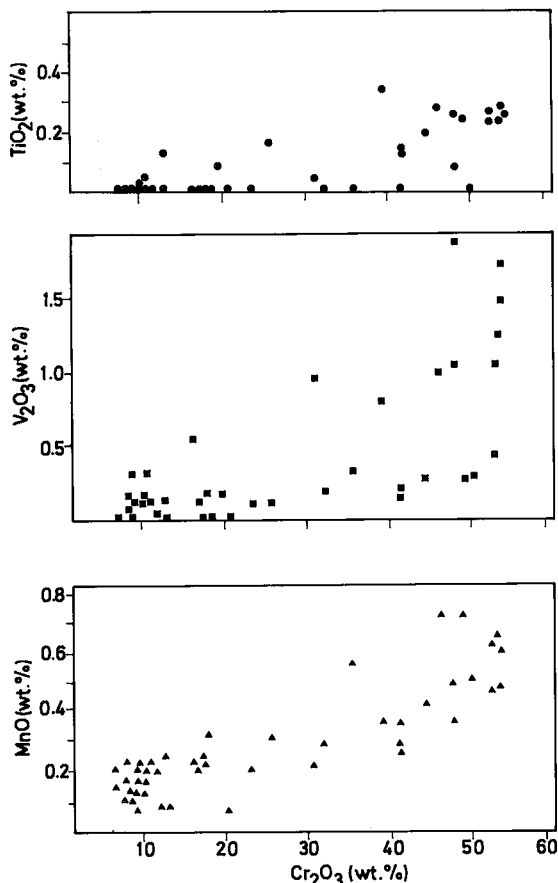


FIG. 20. Plots of Cr₂O₃ versus TiO₂, V₂O₃ and MnO (wt. %) in spinel.

temperatures and with trends from metamorphic and igneous rocks (Engi & Evans 1980) and since the free-energy values for the end-member spinels are not known accurately (Fabriès 1979).

In contrast to the isotherms of Roeder *et al.* (1979) (Fig. 21), those of Fabriès (1979) coincide with the regression line for the olivine-spinel pairs from Thompson. They plot linearly with a correlation coefficient of 0.996 in the $\ln K_D$ - Y_{Cr} diagram (Fig. 21). The regression line lies between the 600 and 800°C isotherms and intersects the 700°C isotherm where Y_{Cr} is 0.17. This may indicate that not all the samples have equilibrated under the same thermal conditions, but some of them, with $Y_{Cr} < 0.17$, have re-equilibrated during progressive metamorphism. Thus, the regression line may represent the path of progressive metamorphism.

The presence of zoned spinel indicates that complete equilibrium between olivine and spinel was not achieved at the high grades. In the $\ln K_D$ - Y_{Cr} diagram, the core composition of two zoned crystals of spinel plots near the 660°C isotherm. If we assume that the olivine is in equilibrium with spinel rims, the assemblage plots very close to the 700°C isotherm (Fig. 21).

Other geotemperature data are obtained from the T-P phase diagram of Gasparik & Lindsley (1980). The diagram is a reconstruction of aluminum solubility in orthopyroxene coexisting with olivine and spinel in the system MgO - Al_2O_3 - SiO_2 after Fujii (1976) and Danckwerth & Newton (1978), and represents an approximation to the model of ideal solution. Extrapolated temperatures using the content of the Mg-Tschermak component (mol. %) in the orthopyroxene solid-solution are approximately 640°C for orthopyroxene coexisting with Mg-Al-spinel. The reason for the low temperature is probably because of the limitation of the geothermometer. This geothermometer in the system Al_2O_3 - MgO - SiO_2 is an approximation to the ideal solid-solution model. According to Danckwerth & Newton (1978), corrections for ideal solution involving FeO and Cr_2O_3 in coexisting spinel species would raise temperature estimates.

PETROGENESIS

As deduced from the mineral assemblages and textures, the ultramafic body has experienced a series of complex hydration and dehydration reactions

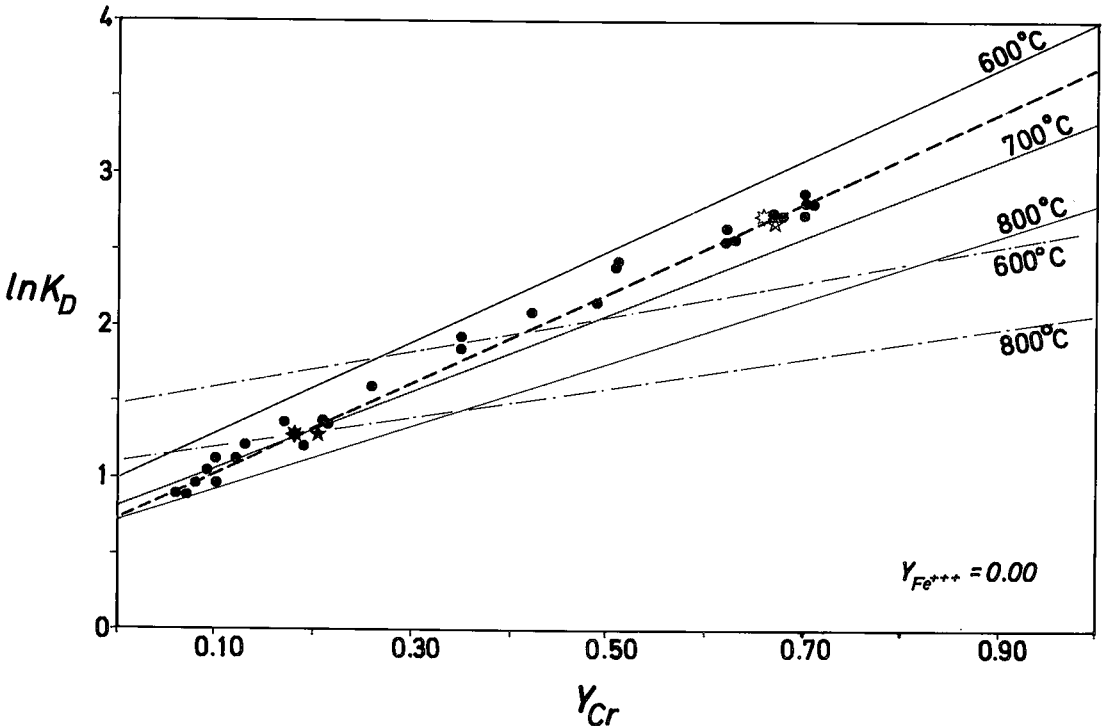


FIG. 21. Plot of $\ln K_D$ versus Y_{Cr} . $K_D = (X_{Mg}/X_{Fe})_{ol} \times (X_{Fe}/X_{Mg})_{sp}$; $Y_{Cr} = Cr/(Cr + Al)$. The composition of two spinel cores (stars) and rims (filled stars) shown for comparison. Dashed line ($2.97 Y_{Cr} - \ln K_D + 0.755 = 0$) is the regression line of plots with a correlation coefficient of 0.996. Solid lines are the isotherms calculated from the equation of Fabriès (1979); dash-dot lines are calculated using the equation of Roeder *et al.* (1979). Precision is within $\pm 50^\circ C$.

before, during and following progressive metamorphism. The dominant mineral assemblage is olivine + tremolite + orthopyroxene + aluminous spinel, suggesting upper-amphibolite-facies conditions. The presence of tremolite as the Ca-bearing silicate instead of diopside and the absence of talc and cordierite constrain the pressure and temperature conditions for the ultramafic rocks in the system $\text{MgO-CaO-Al}_2\text{O}_3\text{-SiO}_2\text{-H}_2\text{O}$ (Fig. 22). The sporadic occurrence of minerals representing lower grades, such as aluminian chromite, chlorite and Ca-poor amphibole, together with olivine and orthopyroxene, may be explained by polymetamorphism or locally varying fluid-phase composition, according to Evans (1977). The fine opaque material may represent relict magnetite stringers formed during serpentinization and enclosed in olivine during deserpentinization, or alternately, it may be a result of high-temperature oxidation of olivine. Since high-temperature products of oxidation usually form more regular patterns (Haggerty & Baker 1967), pyroxene and magnetite usually defining a dendritic intergrowth (Putnis 1979), the former possibility is favored for the formation of the fine opaque material. In addition to

these stringers of relict magnetite, amphibole and chlorite inclusions forming parallel oriented flakes optically continuous with grains adjacent to enclosing olivine megacrysts indicate metamorphic growth of olivine. Similarly, very irregular grain-boundary relations of anhedral olivine with other metamorphic minerals strongly suggest the same. Subhedral and euhedral olivine megacrysts, in part forming a cumulus texture, may be interpreted as recrystallized grains of igneous olivine with minor metamorphic modification. This is supported by the relatively regular content of forsterite in the olivine within individual specimens and uniform MgO-NiO and MgO-MnO relationships in subhedral and euhedral olivine.

Low CaO and Al_2O_3 content of the orthopyroxene megacrysts and their poikiloblastic nature indicate that they are metamorphic, and not igneous relics. Minute inclusions of amphibole, chlorite and phlogopite are similar to the matrix material but smaller in size. They probably resulted from high growth-rate of orthopyroxene relative to the rate of diffusion of components of the inclusions through the host orthopyroxene. According to the phase rela-

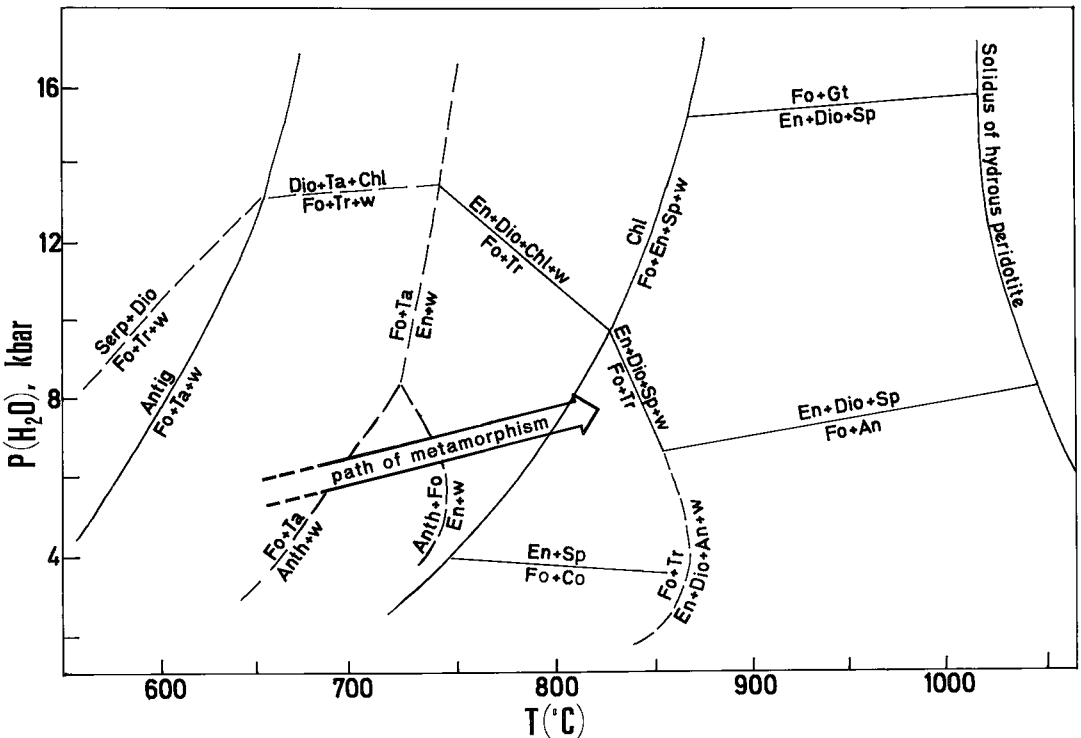


FIG. 22. Phase diagram showing mineral assemblages in ultramafic rocks as a function of temperature and water pressure. Solid lines are experimentally determined curves; dashed lines are theoretical (calculated) curves, after Evans (1977) and Jenkins (1981). Also shown is the interpreted path of metamorphism for ultramafic rocks at the Thompson mine. Abbreviations: Amp amphibole, Anth anthophyllite, Antig antigorite, Chl chlorite, Co cordierite, Dio diopside, En enstatite, Fo forsterite, Gt garnet, Serp serpentine, Sp spinel, Ta talc, Tr tremolite, w water.

tions in Figure 22, enstatite forms from forsterite and anthophyllite at temperatures above 700°C, below 8 kbar pressure.

During progressive metamorphism, spinel changed in composition from Al-chromite through picotite and Cr-spinel to Mg-Al-spinel, as suggested by Evans (1977). Equilibration of coexisting Al-chromite and olivine was probably achieved at approximately 660°C. This opaque Al-chromite changed to a dark brownish red semiopaque variety at its margin, which became more Al- and Mg-rich relative to Cr and Fe during an increase of temperature. Pale brownish yellow and yellowish green spinels, on the other hand, probably formed at temperatures of 685 and 720°C, respectively. Spinel, together with olivine and orthopyroxene, may be formed from chlorite according to the dehydration reaction: $\text{clinochlore} = \text{forsterite} + 2 \text{ enstatite} + \text{spinel} + 4\text{H}_2\text{O}$. This reaction in the system $\text{MgO}-\text{CaO}-\text{Al}_2\text{O}_3-\text{SiO}_2-\text{H}_2\text{O}$ (Evans 1977, Jenkins 1981) takes place between 750 and 825°C at 4–9 kbar pressure. The upper-pressure limit was estimated from the intersection of the reaction above with the reaction $\text{Fo} + \text{Tr} = \text{En} + \text{Dio} + \text{Sp} + \text{w}$ (Fig. 22), whereas the lower limit was estimated from the reaction $\text{En} + \text{Sp} = \text{Fo} + \text{Co}$. Addition of iron into this 5-component system, however, shifts the reaction curves toward lower temperatures. Furthermore, reaction boundaries in the system will be shifted to lower temperatures and pressures if the activity of H_2O in the ambient fluid is not close to unity (Jenkins 1981). As a result, a temperature of approximately 720°C, obtained from Mg-Al-spinel and olivine pairs, would be realistic for the formation of spinel. Anhedral inclusions of chlorite (chromium-bearing clinochlore), which developed along certain crystallographic directions in the host olivine, are interpreted as a product of the reaction between the host olivine and spinel inclusions (Fig. 10).

Serpentinization seen in zones 2 and 6 is a late-stage event, developed following metamorphism and deformation. This is indicated by thin veins of serpentine cutting olivine neoblasts as well as other metamorphic minerals. On the margin of the body (zone 12), recrystallized phlogopite is later replaced by a green chlorite pseudomorph.

Deformation of the body is indicated by the fabric, kink banding and undulatory extinction of olivine and orthopyroxene megacrysts. According to Poirier & Nicolas (1975), spinel in peridotite nodules is progressively scattered with increasing flow since it is less ductile than the silicates. By their interpretation, the scatter seen in Mg-Al-spinel may be due to increasing deformation. However, the situation is different in zone 5b, where the spinel is Al-chromite occupying the interstices of olivine megacrysts. This zone is probably the least deformed part of the body.

This fact is further supported by the unrecrystallized grains of olivine.

Recrystallization accompanied or followed deformation. It seems to have been an annealing or static type of recrystallization because of the large grain-size, equant grain-shapes, polygonal grain-boundaries, and absence of features of intragranular strain (Green *et al.* 1970), as opposed to inequant grain-shapes and strong preferred orientation, which are characteristics of syntectonic recrystallization. The presence of a bimodal texture seen in zone 5a, however, suggests that recrystallization is syntectonic (Goetze 1975). If this is the case, some features such as equant and large grain-size may have been formed with the help of a small amount of water (Green *et al.* 1970) during the recovery stage. The driving force for the type of recrystallization that developed along grain boundaries and dislocations of the olivine megacrysts is probably strain energy stored in megacrysts. On the other hand, the driving force for the recrystallization that resulted in the formation of equigranular olivine mosaic is more likely grain-boundary and surface energy.

CONCLUSIONS

The ultramafic rocks in the Thompson mine were altered prior to metamorphism, as indicated by 1) relict magnetite stringers in olivine megacrysts, 2) parallel oriented amphibole and chlorite flakes in olivine megacrysts, and 3) abundant minute inclusions of amphibole, chlorite and phlogopite in orthopyroxene megacrysts.

Olivine megacrysts may have recrystallized from partly altered olivine during progressive metamorphism. Orthopyroxene may have formed at the expense of olivine and (probably) anthophyllite at temperatures above 700°C.

Mg- Fe^{2+} partitioning between olivine and Al-chromite was blocked at 670°C. Formation of a more Al- and Mg-rich margin relative to the Cr- and Fe-rich core in spinel probably took place at higher grades during progressive metamorphism. This could be considered as a partial re-equilibration, in terms of an Mg- Fe^{2+} exchange reaction between olivine and spinel at higher temperatures.

Temperatures estimates and the mineral assemblage of olivine + tremolite + orthopyroxene + Al-spinel correspond to the upper amphibolite facies of metamorphism. During or following metamorphism, the ultramafic body was deformed and subsequently recrystallized.

Locally developed secondary serpentinization is the latest event observed. This secondary serpentinization probably corresponds to the extensive serpentinization of the peridotitic rocks elsewhere in the belt.

ACKNOWLEDGEMENTS

This work was done as part of a Ph.D. thesis under the supervision of Dr. G. Armbrust. The research was supported by a grant from the University of Ottawa and a scholarship from the Mineral Research and Exploration Institute of Turkey (MTA). Inco Metals Ltd., Manitoba Division, supported field work. The author is greatly indebted to Dr. W. Peredery for suggesting the topic and for his generous help in the field. Drs. R. Kretz, W. Peredery and R. F. Emslie reviewed the earlier version of the paper and gave constructive suggestions. The final version of the paper was reviewed by Drs. C. Pride and O. R. Eckstrand.

REFERENCES

- ARAI, S. (1975): Contact metamorphosed dunite-harzburgite complex in the Chugoku district, western Japan. *Contr. Mineral. Petrology* **52**, 1-16.
- BLISS, N.W. (1973): *A Comparative Study of Two Ultramafic Bodies at the Southwest End of the Manitoba Nickel Belt, with Special Reference to the Chromite Mineralogy*. Ph.D. thesis, McGill Univ., Montreal, Que.
- CHAMPNESS, P.E. (1970): Nucleation and growth of iron oxides in olivines. *Mineral. Mag.* **37**, 790-800.
- COATS, C.J.A. (1966): *Serpentinized Ultramafic Rocks of the Manitoba Nickel Belt*. Ph.D. thesis, Univ. Manitoba, Winnipeg, Man.
- CRANSTONE, D.A. & TUREK, A.T. (1976): Geological and geochronological relationships of the Thompson nickel belt, Manitoba. *Can. J. Earth Sci.* **13**, 1058-1069.
- DANCKWERTH, P.A. & NEWTON, R.C. (1978): Experimental determination of the spinel peridotite to garnet peridotite reaction in the system MgO-Al₂O₃-SiO₂ in the range 900°C-1100°C and Al₂O₃ isopleths of enstatite in the spinel field. *Contr. Mineral. Petrology* **66**, 189-201.
- DEER, W.A., HOWIE, R.A. & ZUSSMAN, J. (1966): *An Introduction to the Rock-Forming Minerals*. Longman, London.
- DOBRETsov, N.L. (1968): Paragenetic types and compositions of metamorphic pyroxenes. *J. Petrology* **9**, 358-377.
- ENGI, M. & EVANS, B.W. (1980): A re-evaluation of the olivine-spinel geothermometer: discussion. *Contr. Mineral. Petrology* **73**, 201-203.
- EVANS, B.W. (1977): Metamorphism of alpine peridotite and serpentinite. *Ann. Rev. Earth Planet. Sci.* **5**, 397-447.
- _____ & FROST, B.R. (1975): Chrome-spinel in progressive metamorphism - a preliminary analysis. *Geochim. Cosmochim. Acta* **39**, 959-972.
- _____ & TROMMSDORFF, V. (1974): Stability of enstatite + talc, and CO₂-metasomatism of metaperidotite, Val d'Efra, Lepontine Alps. *Amer. J. Sci.* **274**, 274-296.
- FABRIÈS, J. (1979): Spinel-olivine geothermometry in peridotites from ultramafic complexes. *Contr. Mineral. Petrology* **69**, 329-336.
- FROST, B.R. (1975): Contact metamorphism of serpentinite, chloritic blackwall and rodingite at Paddy-Go-Easy Pass, Central Cascades, Washington. *J. Petrology* **16**, 272-313.
- FUJII, T. (1976): Solubility of Al₂O₃ in enstatite coexisting with forsterite and spinel. *Carnegie Inst. Wash. Yearbook* **75**, 566-571.
- GASPARIK, T. & LINDSLEY, D.H. (1980): Phase equilibria at high pressure of pyroxenes containing monovalent and trivalent ions. In *Pyroxenes* (C. T. Prewitt, ed.). *Mineral. Soc. Amer., Rev. Mineral.* **7**, 309-339.
- GOETZE, C. (1975): Sheared lherzolites: from the point of view of rock mechanics. *Geology* **3**, 172-173.
- GREEN, H.W., GRIGGS, D.T. & CHRISTIE, J.M. (1970): Synthetic and annealing recrystallization of fine grained quartz aggregates. In *Experimental and Natural Rock Deformation* (P. Paulitsch, ed.). Springer-Verlag, New York.
- HAGGERTY, S.E. & BAKER, I. (1967): The alteration of olivine in basaltic and associated lavas. I. High temperature alteration. *Contr. Mineral. Petrology* **16**, 233-257.
- IRVINE, T.N. (1965): Chromian spinel as a petrogenetic indicator. I. Theory. *Can. J. Earth Sci.* **2**, 648-672.
- JACKSON, E.D. (1969): Chemical variation in coexisting chromite and olivine in the chromite zones of the Stillwater Complex. In *Magmatic Ore Deposits* (H.D.B. Wilson, ed.). *Econ. Geol., Mon.* **4**, 41-71.
- JAMIESON, R.A. (1981): Metamorphism during ophiolite emplacement - the petrology of the St. Anthony Complex. *J. Petrology* **22**, 397-449.
- JENKINS, D.M. (1981): Experimental phase relations of hydrous peridotites modelled in the system H₂O-CaO-MgO-Al₂O₃-SiO₂. *Contr. Mineral. Petrology* **77**, 166-176.
- MEDARIS, L.G. (1969): Partitioning of Fe⁺⁺ and Mg⁺⁺ between coexisting synthetic olivine and orthopyroxene. *Amer. J. Sci.* **267**, 945-968.

- MERCIER, J.-C. C. (1976): Single pyroxene geothermometry and geobarometry. *Amer. Mineral.* **61**, 603-615.
- _____ & NICOLAS, A. (1975): Textures and fabrics of upper-mantle peridotites as illustrated by xenoliths from basalts. *J. Petrology* **16**, 454-487.
- PEREDERY, W.V. (1979): Relationship of ultramafic amphibolites to metavolcanic rocks and serpentinites in the Thompson belt, Manitoba. *Can. Mineral.* **17**, 187-200.
- _____ (1982): Geology and nickel sulphide deposits of the Thompson belt, Manitoba. In *Precambrian Sulphide Deposits* (R.W. Hutchinson, C.D. Spence & J.M. Franklin, eds.). *Geol. Assoc. Can., Robinson Vol.*, 165-209.
- PETERS, T. (1968): Distribution of Mg, Fe, Al, Ca and Na in coexisting olivine, orthopyroxene and clinopyroxene in the Totalp serpentinite (Davos, Switzerland) and in the Alpine metamorphosed Malenco serpentinite (N. Italy). *Contr. Mineral. Petrology* **18**, 65-75.
- POIRIER, J.P. & NICOLAS, A. (1975): Deformation-induced recrystallization due to progressive misorientation of subgrains, with special reference to mantle peridotites. *J. Geol.* **83**, 707-720.
- PUTNIS, A. (1979): Electron petrography of high-temperature oxidation in olivine from the Rhum layered intrusion. *Mineral. Mag.* **43**, 293-296.
- ROEDER, P.L., CAMPBELL, I.H. & JAMIESON, H.E. (1979): A re-evaluation of the olivine-spinel geothermometer. *Contr. Mineral. Petrology* **68**, 325-334.
- RUSSELL, J.K. (1981): Metamorphism of the Thompson nickel belt gneisses: Paint Lake, Manitoba. *Can. J. Earth Sci.* **18**, 191-209.
- SABOIA, L.A. (1978): *The West Manasan and the Pipe Mine: 2 Ultramafic Bodies of the Thompson Nickel Belt*. M.Sc. thesis, Univ. Western Ontario, London, Ont.
- SACK, R.O. (1980): Some constraints on the thermodynamic mixing properties of Fe-Mg orthopyroxenes and olivines. *Contr. Mineral. Petrology* **71**, 257-269.
- SMITH, D.G.W. & GOLD, C.M. (1979): EDATA2: a Fortran IV computer program for processing wavelength- and/or energy-dispersive electron microprobe analysis. In *Proc. Microbeam Anal. Soc.*, 14th Ann. Conf. (San Antonio; D.E. Newbury, ed.), 273-278.
- TROMMSDORFF, V. & EVANS, B.W. (1974): Alpine metamorphism of peridotitic rocks. *Schweiz. Mineral. Petrog. Mitt.* **54**, 333-352.
- _____ & _____ (1980): Titanian hydroxylclinohumite: formation and breakdown in antigorite rocks (Malenco, Italy). *Contr. Mineral. Petrology* **72**, 229-242.
- VANCE, J.A. & DUNGAN, M.A. (1977): Formation of peridotites by deserpentinization in the Darrington and Sultan areas, Cascade Mountains, Washington. *Geol. Soc. Amer. Bull.* **88**, 1497-1508.
- WEBER, W. & SCOATES, R.F.J. (1978): Archean and Proterozoic metamorphism in the northwestern Superior Province and along the Churchill-Superior boundary, Manitoba. In *Metamorphism in the Canadian Shield* (J.A. Fraser & W.W. Heywood, eds.). *Geol. Surv. Can. Pap.* **78-10**, 5-16.
- ZURBRIGG, H.F. (1963): Thompson Mine geology. *Can. Inst. Mining Metall. Bull.* **56**, 451-460.

Received May 20, 1983, revised manuscript accepted August 1, 1983.